



BNL-90849-2009-CP

***Effect of Te Inclusions on Internal Electric Field of
CdMnTe Gamma-Ray Detectors***

**Oluseyi Babalola, Aleksey Bolotnikov, Stephen Egarievwe, Anwar
Hossain, Arnold Burger, and Ralph James**

*Presented at the SPIE Optics and Photonics
San Diego, CA
August 2-6, 2009*

December 2009

**Nonproliferation and National Security Department
Detector Development and Testing Division**

Brookhaven National Laboratory

P.O. Box 5000
Upton, NY 11973-5000
www.bnl.gov

Notice: This manuscript has been authored by employees of Brookhaven Science Associates, LLC under Contract No. DE-AC02-98CH10886 with the U.S. Department of Energy. The publisher by accepting the manuscript for publication acknowledges that the United States Government retains a non-exclusive, paid-up, irrevocable, world-wide license to publish or reproduce the published form of this manuscript, or allow others to do so, for United States Government purposes.

This preprint is intended for publication in a journal or proceedings. Since changes may be made before publication, it may not be cited or reproduced without the author's permission.

DISCLAIMER

This report was prepared as an account of work sponsored by an agency of the United States Government. Neither the United States Government nor any agency thereof, nor any of their employees, nor any of their contractors, subcontractors, or their employees, makes any warranty, express or implied, or assumes any legal liability or responsibility for the accuracy, completeness, or any third party's use or the results of such use of any information, apparatus, product, or process disclosed, or represents that its use would not infringe privately owned rights. Reference herein to any specific commercial product, process, or service by trade name, trademark, manufacturer, or otherwise, does not necessarily constitute or imply its endorsement, recommendation, or favoring by the United States Government or any agency thereof or its contractors or subcontractors. The views and opinions of authors expressed herein do not necessarily state or reflect those of the United States Government or any agency thereof.

EFFECT OF TE INCLUSIONS ON INTERNAL ELECTRIC FIELD OF CdMnTe GAMMA-RAY DETECTORS

Oluseyi Stephen Babalola^{1,2,3}, Aleksey E. Bolotnikov², Stephen U. Egariyev², Anwar M. Hossain², Arnold Burger³, Ralph B. James²

1. Vanderbilt University, Nashville, TN.
2. Brookhaven National Laboratory, Upton, NY.
3. Fisk University, Nashville, TN

Abstract

We studied two separate as-grown CdMnTe crystals by Infrared (IR) microscopy and Pockels effect imaging, and then developed an algorithm to analyze and visualize the electric field within the crystals' bulk. In one of the two crystals the size and distribution of inclusions within the bulk promised to be more favorable in terms of efficiency as a detector crystal. However, the Te inclusions were arranged in characteristic 'planes'. Pockels imaging revealed an accumulation of charges in the region of these planes. We demonstrated that the planes induced stress within the bulk of the crystal that accumulated charges, thereby causing non-uniformity of the internal electric field and degrading the detector's performance.

Introduction

CdMnTe (CMT) is an attractive material for room-temperature nuclear detectors that potentially might replace CdZnTe crystals [1-4] due to its advantageously wider bandgap energy that is tunable with Mn concentration, high resistivity, good electron-transport properties and near-unity segregation coefficient that promises a homogeneous Mn distribution in CMT matrix and results in growth of more uniform and larger CMT single crystals [5-7].

However, in present-day CMT crystals the high concentrations of defects limit their performance. It is noteworthy that the major problem in realizing detector-grade CMT crystals is the lack of pure commercial Mn used for growing the crystals. Mn usually is supplied as 99.99% pure compared to Zn in CZT that offers up to 99.99999% purity. Also, CMT crystals contain high concentrations of twins and twin boundaries that are profusely decorated by Te inclusions and precipitates. Te inclusions in CdTe crystals represent the solidified Te-rich melt captured at the interface of crystal growth due to morphological instabilities and incorporated into the ingot [8]. Often they are ≥ 1 microns [9-11], and, at larger sizes, can distort the internal electric field and also act as charge traps thereby degrading the detector's performance. A uniform distribution of the internal electric field in a detector is essential for good collection efficiency and resolution. In a recent paper, we presented our study of the internal electric field in CMT crystals, showing how the observed characteristic planes of Te inclusions deteriorate the CMT detector performance.

This work describes the applications of our Pockels-effect technique to study such defects in the crystals, and introduces an algorithm we developed for visualizing and analyzing the Pockels images. We detail and explain the effects of Te inclusion planes, which are

responsible for inducing stress in the crystals, on the internal electric field at different biases.

Pockels electro-optic effect and algorithm

Figure 1 shows that CMT, like zinc-blende crystals, exhibits induced birefringence in the presence of an electric field in which the refractive index is modified anisotropically in the transverse plane [12, 13]. Incident linearly polarized light is filtered with a 1060nm narrow-band filter and passed through a polarizer with the E vector oriented 45° with respect to the applied electric field, and then traverses the crystal and finally crosses through an analyzer on to a CCD camera. The polarized ray, in passing through a medium with modified refractive index, splits into an ordinary ray and an extraordinary ray parallel to the optical axis.

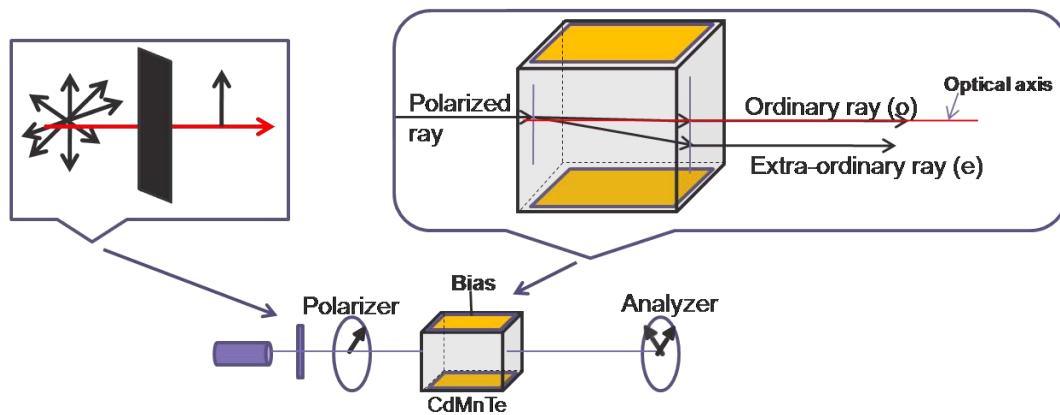


Figure 1 Schematic diagram of Pockels-effect imaging.

The resultant of these two rays determines the intensity of the transmitted light, I , that depends on the direction of the analyzer relative to the polarizer and the presence and magnitude of the applied bias. Figure 2 shows the resultant condition, and hence, the magnitude of transmitted light at different conditions. The intensities of both the transmitted light when detector is biased and the maximum intensity with an unbiased detector (I_0) is related to the electric field according to the equation below:

$$I = I_0 \sin^2 \left(\frac{\pi n_o^3 r d}{\lambda} E \right)$$

where d is the optical-path's length (thickness of crystal), r is the linear electro-optic coefficient, n_o is the field free refractive index, λ is the wavelength of incident light, and E is the average electric field.

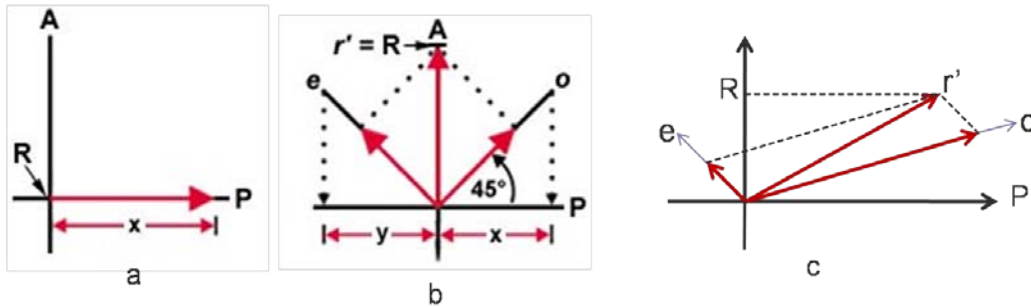


Figure 2 Intensity of transmitted light as the resultant of ordinary- and extraordinary-rays with respect to the direction of analyzer relative to polarizer. (a). Optical axis 45° to polarizer P that is parallel to analyzer A gives the maximum intensity when no bias is applied. (b). P transverse to A, where light passing through the crystal vibrates in a plane parallel to P; no applied bias. Light is cross-polarized and does not pass through. (c). Cross-polarized with bias applied. The electric field induces birefringence.

Experiment

An algorithm was written in the Interactive Data Language (IDL) development environment for analyzing the Pockels images and visualizing the internal electric field. As the flowchart in figure 3 illustrates, the algorithm entails five main processes.

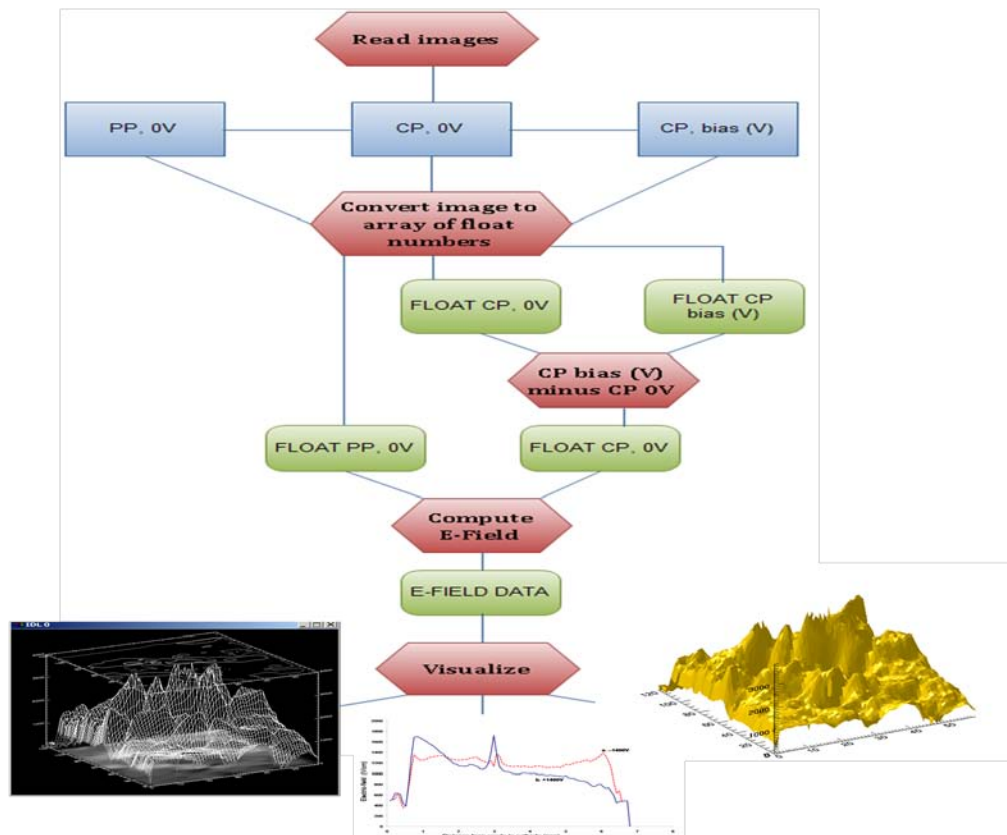


Figure 3 IDL algorithm for analyzing and visualising the internal electric field in CMT crystals

The images first are read into the IDL environment, and the attributes of a display window defined.

Next, the images are converted to floating point arrays. For each image, two vectors are constructed containing the x and y position, respectively, of the array. Then, a bilinear interpolation of the image values is created. Thereafter, the vectors representing the biased crystals are subtracted from those for unbiased crystals with cross-polarized transmitted light, and finally, the internal electric field is computed and visualized.

We studied two $6 \times 6 \times 12 \text{ mm}^3$ CMT crystals cut from two different ingots (CMT A and CMT B) with different amounts of indium doping (4 ppm and 2.5 ppm respectively) in this experiment. The crystals were polished mechanically with Al_2O_3 abrasive papers with decreasing grit sizes and then finally were polished with a 0.05-micron alumina slurry. The crystals were etched with 2% Bromine-Methanol (BM), cleaned with methanol, and dried in nitrogen gas to remove any etching residue. We studied the crystals with our infrared (IR) microscopy system, described elsewhere [14]. We selected the crystal from the second ingot, CMT B, that contained twins decorated by Te inclusions as the most suitable for internal electric-field profiling employing the Pockels effect. Gold contacts were deposited on its planar surfaces using RF sputtering in argon gas. We measured current-voltage and the Pockels effect on the fabricated detector.

Results and discussion

Figure 4 shows IR images of both crystals. CMT A has a higher concentration of Te inclusions than CMT B. Also, the sizes of Te inclusions in CMT A are much larger than those in CMT B. By counting with another IDL algorithm reported in [15] we found that the inclusions in the crystals from ingot A are two orders-of-magnitude larger than those in the crystals from ingot B.

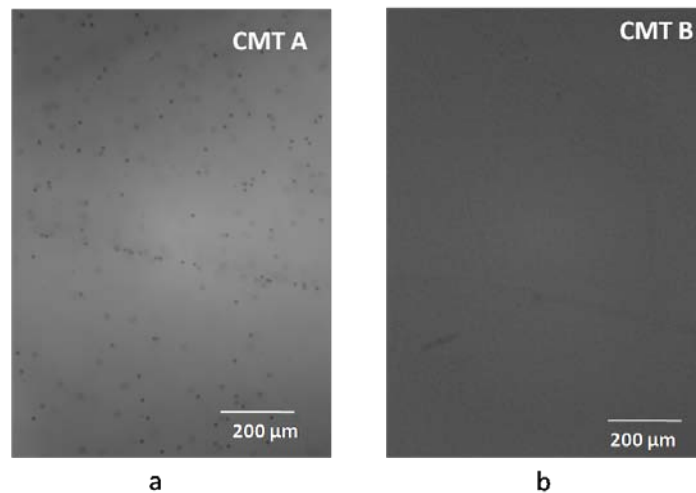


Figure 4 IR images of CMT crystals, showing that CMT A (a) has more and larger Te inclusions than CMT B (b).

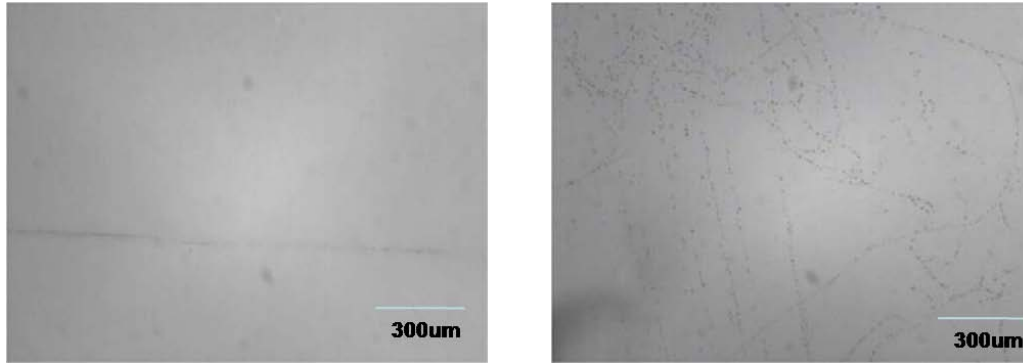


Figure 5 IR images of CMT B a) view from the side, along (111) showing a thin plane of Te inclusions. b) view of the same position from the top showing the Te inclusions that form the plane

We observed characteristic parallel planes of Te inclusions in CMT B representing twins and twin boundaries. One of such planes, shown in Figure 5, was chosen for internal electric-field profiling. Accordingly, we fabricated the CMT B crystal into a $6 \times 6 \times 6 \text{ mm}^3$ planar detector following the steps described earlier, ensuring that it featured the plane of Te inclusions. Figure 6 shows the Pockels images at zero bias. Figure 6a is an infrared image at zero bias showing the thin plane formed by Te inclusions; Figure 6b is a cross-polarized image also at zero bias, revealing the stress induced within the crystal by this plane. We note that the plane of Te inclusions is barely visible in Figure 7a, but it becomes more apparent with increased bias, as observed in figures 7b, c, and d, verifying that the line in figure 6b represents induced stress around the region of the Te inclusion plane, while the lines in figure 7 are due to the build-up of the electric field around these planes.

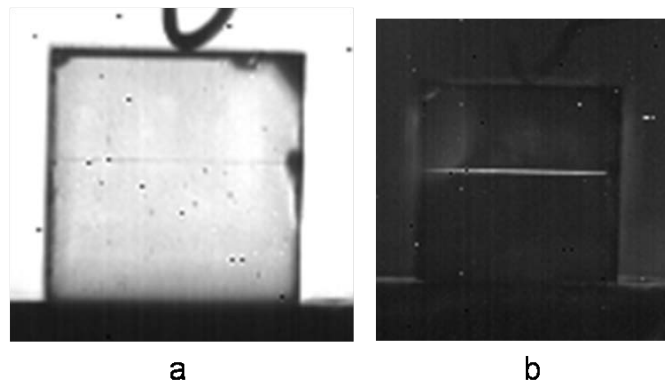


Figure 6 Pockels images of CMT B at zero bias obtained for a) parallel linear-polarization; b) cross-linear polarization

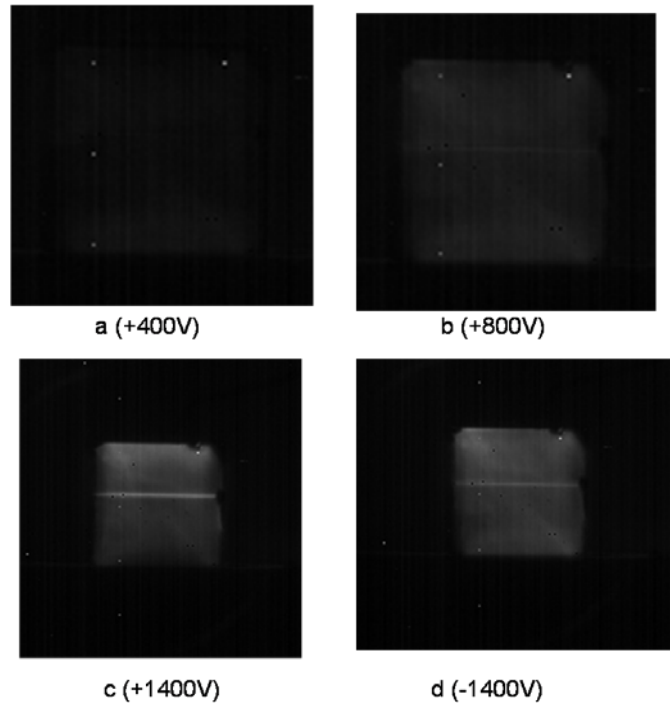


Figure 7 Pockels images of CMT B with cross-linear polarization at applied biases of a) +400V, b) +800V, c) +1400V, and d) -1400V .

Using the IDL algorithm described above, figure 8 visualizes the 3-dimensional distribution of electric field for both a positive- and a negative-1400V applied bias. The region of Te inclusion plane is evident as a non-uniformity in the electric-field distribution due to charge accumulation and buildup within region of the Te inclusion plane. Earlier, we showed that this charge buildup can cause the performance of CMT nuclear detectors to deteriorate.

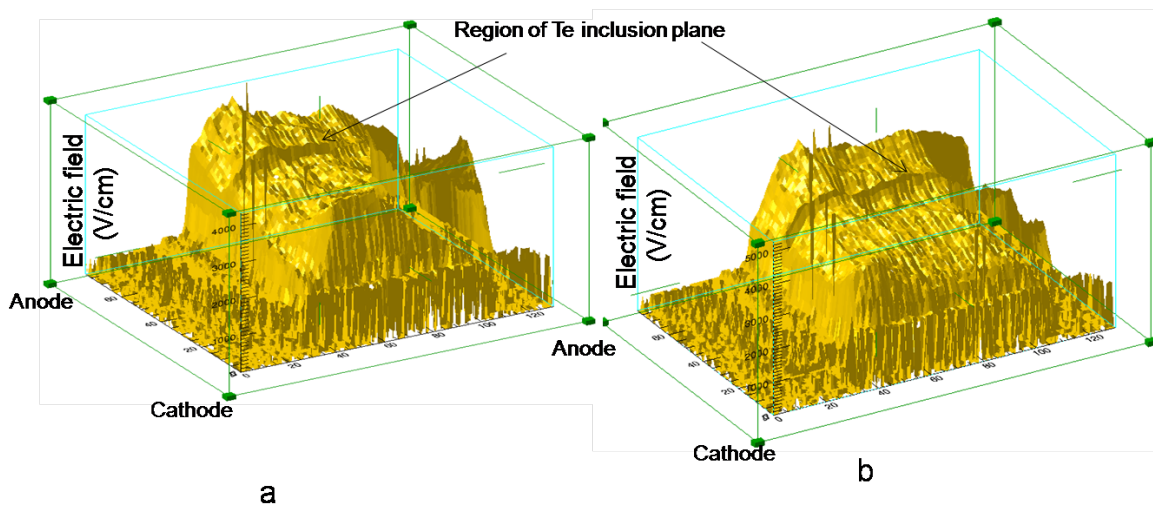


Figure 8 Electric field distribution within the bulk of CMT B at an applied bias of a) +1400V, b) -1400V .

Conclusions

We explored CMT crystals from two ingots with IR imaging that revealed a characteristic plane of Te inclusions in one of them. The effect of this twin plane on the internal electric field of the crystal was studied by employing the Pockels effect. We demonstrated that the plane induces stress in the CMT crystal, and distorts its internal electric-field. We developed an algorithm to verify the three-dimensional distribution of the electric-field in the bulk of the CMT crystal; the distortion of this internal electric field reduces the crystal's detection abilities, such as its charge collection efficiency. Finally, our algorithm for electric field visualization might be applied advantageously to screen out poor detectors based on the internal electric field profile.

Acknowledgement

This work was supported by U.S. Department of Energy, Office of Nonproliferation Research and Development, NA-22.

References

1. A. Burger, K. Chattopadhyay, H. Chen, J. O. Ndap, X. Ma, S. Trivedi, S. W. Kutcher, R. Che, and R. Rosemeier. *J. Crystal Growth* 198/19 (1999) 872.
2. A. Mycielski, A. Burger, M. Sowinska, M. Groza, A. Szadkowski, P. Wojnar, B. Witkowska, W. Kaliszek, and P. Siffert, *Phys. Stat. Sol. (c)* 2, No. 5, (2005) 1578.
3. A. Hossain, Y. Cui, A. e. Bolotnikov, G. S. Camarda, G. Yang, D. Kochanowska, M. Witkowska-baran, A. Mycelski and R. B. James ,Vanadium-doped CMT crystals as X- and gamma ray detectors. *J Electronic Materials*. (2009) *In Press*.
4. G. A. Brost, K. M. Magde, S. Trivedi, *Opt. Mater.* 4 (1995), 224.
5. U. Hommerich, X. Wu, V. R. Davis, S.B. Trivedi, K. Grasza, R. J. Chen, S. Kutcher, *Opt. Lett.* 22 (15) (1997) 1180.
6. Y. R. Lee and A. K. Ramdas, *Solid State Commun.* 51 (1984) 861.
7. A. Y. Wu and R. J. Sladek, *J. Appl. Phys.* 53 (1982) 8589.
8. Y. Wang, K. Kudo, Y. Inatomi, R. Ji, T. Motegi. *J. Crys. Gr.* 284 (2005) 406
9. J. Gonzales-Hernandez, E. Lopez-Cruz, D. D. Allred, and W. P. Allred, *J. Vac. Sci. Technol. A* 8 (4), (1990) 3255.
10. P. De Antonis, E. J. Morton, and F. J. W. Podd, *IEEE Trans. Nucl. Sci.* 43, no. 3, (1996) 1487.
11. P. Rudolph, M. Neubert and M. Miihlberg. *J Crystal Growth* 128 (1993) 582.
12. H. W. Yao, R. J. Anderson, R. B. James, and R. W. Olsen, *Proc. Materials Research Society Symp.* Vol. 487, (1998) 51.
13. A. Zumbiehl, M. Hage-Ali, P. Fougeres, J. M. Koebel, R. Regal, and P. Siffert, *J. Crystal Growth* 197, (1999) 650.
14. G. S. Camarda, A. E. Bolotnikov, G. A. Carini, Y. Cui, K. T. Kohman, L. Li, R. B. James, *Proceedings of SPIE Conf. Hard X-ray and gamma-ray detector physics and penetrating radiation systems.* Vol. 6319, (2006) 63190Z.1.
15. O.S. Babalola, A. E. Bolotnikov, M. Groza, A. Hossain, S. Egarievwe, R.B. James and A. Burger. *J.Crys. Gr.* Vol 311, 14, (2009) 3702.